

First-Principles Study on Dielectric Response of Amorphous Al₂O₃

Hiroyoshi Momida, Takenori Yamamoto, Tomoyuki Hamada,

Yoshiteru Takagi, Tsuyoshi Uda* and Takahisa Ohno**

Institute of Industrial Science, University of Tokyo, 4-6-1 Komaba, Meguro, Tokyo 153-8505, Japan

* AdvanceSoft Corporation, 4-6-1 Komaba, Meguro, Tokyo 153-8904, Japan

** National Institute for Materials Science, 1-2-1 Sengen, Tsukuba, Ibaraki 305-0047, Japan

Dielectric response of amorphous Al₂O₃ has been investigated using a first-principles calculation. Calculated structural properties, such as density of mass and atomic coordination number, agree with experimental values in the amorphous states. Calculated dielectric constant is also close to observed values. We especially focus attention on what kind of local atomic environment makes large contribution to the dielectric constant due to lattice polarization, and found that there are few atomic sites leading to the high dielectric constant via low-frequency lattice vibration mode.

Key words: amorphous structure, Al₂O₃, dielectric response, first-principles calculation.

1. INTRODUCTION

Amorphous alumina (a-Al₂O₃) is one of the promising materials as new gate dielectric layer in next generation complementary metal-oxide semiconductor (CMOS) transistor. This is because of its high dielectric constant relative to that of amorphous SiO₂ and SiON used currently. It is experimentally known that the amorphous structure on the Si substrate is thermally stable comparing with other candidate materials, such as HfO₂, even at high annealing temperature (about 1000K) during the CMOS fabrication process [1]. The stability of the amorphous structure is important to avoid unfavorable problems, such as crystal domain segregation and anisotropy of dielectric response.

Hafnium aluminate (HfO₂-Al₂O₃) have been also attracted much interest as the CMOS dielectric, because of its higher dielectric constant than that of the a-Al₂O₃. Several researchers have tried to optimize the Hf content, and it is empirically known that the Hf content of 20% - 40% seems to be best choice for dielectric constant and thermal stability enhancement of the amorphous structure [1,2,3]. However, microscopic origin of the higher dielectric constant due to the Hf inclusion in an Al₂O₃ matrix is still unknown, even for the system with low Hf content.

Recently, we have investigated the dielectric response of candidate CMOS gate materials, called high-k materials, such as Al₂O₃, HfO₂, CeO₂ and so on in the crystal phase [4]. It has been shown that a first-principles calculation well reproduce observed dielectric constant. In these high-k materials, the contribution of lattice polarization is much larger than electron one. Thus, in order to understand the experimental facts for a-Al₂O₃ and a-HfO₂-Al₂O₃, microscopic relation between the dielectric constant and the lattice polarization should be clarified. Detailed information about the amorphous structure and its electronic structure are needed for the understanding.

In this study, dielectric response of a-Al₂O₃ is studied by a first-principles calculation. The amorphous model structure is theoretically calculated, and its electronic

structure is investigated. Calculated density of mass, coordination number and electronic band gap, are compared with experimental values. Dielectric constant of the a-Al₂O₃ model is calculated, and is analyzed by focusing on lattice polarization effect that makes larger contribution than electron one.

2. METHOD OF CALCULATION

Electronic structure and dielectric response are calculated by means of a first-principles method. Calculations are based on density functional theory (DFT) within local density approximation (LDA) [5,6,7]. One-electron Kohn-Sham equations are solved self-consistently by using plane wave pseudo-potential (PWPP) method [8,9]. Program packages "CIAO" and "PHASE" are used for pseudo-potential preparation and DFT-PWPP calculations, respectively [10]. We use cutoff energy of 25 Ry (225 Ry) for Kohn-Sham wavefunction (electron density and potential), and the electronic structure is calculated for a wave vector of Γ point in a Brillouin zone.

In order to model the amorphous structure, we firstly perform classical molecular dynamics (MD) calculations of Al₂O₃, using the empirical pair potential by Matsui [11]. We used program package "FOTTAS" [10]. The MD calculations are performed under NPT condition [12,13,14] with a rectangular unit cell, and a MD time interval is set at 1.0 fs. It is expected that amorphous structures are obtained by a melt-and-quench technique, as already reported for a-Al₂O₃ with large number of atoms (more than 1000 atoms) [15,16,17]. Generally, crystal phase is known to be realized with much slow cooling rate from liquid, while an amorphous phase is known to be obtained with relatively fast cooling rate in MD calculation. In this study, the liquid state is calculated at 3000K for the initial MD structure with 60 - 120 atoms in its unit cell. We analyze the structure averaged over final 4.0 ps at 300 K. For the obtained structures, the atomic positions are optimized again by a first-principles DFT calculation with fixed density (unit cell length) until all atomic force becomes less than 1

mRy/Bohr.

Dielectric response to static external field originates from electron and lattice polarization as the main contributions. The electron contribution ($\epsilon_{\alpha\beta}^{\text{ele}}$, α and β stand for a coordinate) can be obtained by calculating direct inter-band transition moments in a Brillouin zone, as described from a perturbation theory [18]. The lattice contribution ($\epsilon_{\alpha\beta}^{\text{lat}}$) is described as

$$\epsilon_{\alpha\beta}^{\text{lat}} = \frac{4\pi e^2}{V_{\text{cell}}} \sum_{\lambda} \frac{Z_{\lambda\alpha}^* Z_{\lambda\beta}}{\omega_{\lambda}^2},$$

where mode effective charge vector $Z_{\lambda\alpha}^*$ of λ -th normal mode is defined as

$$Z_{\lambda\alpha}^* = \sum_{i,\beta} Z_{i,\alpha\beta}^* \xi_{\lambda,i,\alpha}.$$

Here, $Z_{i,\alpha\beta}^*$ is the Born effective charge tensor of i -th atom calculated by so-called Berry phase method [19,20]. ω_{λ} and $\xi_{\lambda,i,\alpha}$ stand for the lattice vibration frequency and its eigen-displacement; those are calculated by solving an eigenvalue problem of dynamical matrix within a frozen phonon approximation.

3. RESULTS AND DISCUSSION

3.1 Amorphous Structure

First of all, we summarize classical MD results. By performing melt-and-quench MD with several cooling rate (-0.03 - -0.54 K per a time step) for two types of initial MD structure (α - Al_2O_3 crystal, and its final MD structure again), we get two kind of the final structures; one is amorphous like (as shown in Fig.1) and the other one is crystal like at 300 K. The calculated amorphous structures have lower density and averaged coordination numbers (3.02 - 3.38 g/cm^3 and 4.02 - 4.63 at Al) than those in crystals (e.g. 3.99 g/cm^3 and 6.0 at Al for α -phase, 3.66 g/cm^3 and 5.4 at Al for γ -phase from experiments). Calculated values are in good agreement with the reported experimental values (3.05 - 3.40 g/cm^3 and 4.1 - 4.8 at Al) for a- Al_2O_3 [21]. In the MD results, we cannot find the large difference between the amorphous models with 60 and 120 atoms. Calculated coordination number and bond length (discussed later) are also consistent with previous MD studies reported by Kaneta and Yamasaki *et al.* [15,16] and those by Gutiérrez *et al.* [17] using large number of atoms.

Note that the crystal like structures have a high density (3.7 - 3.8 g/cm^3) and coordination number (5.2 - 5.6 at Al), being similar to the crystal values. The crystallized models have periodic distinct peaks in the radial distribution function, showing the lattice-formed atomic structure.

The first-principles re-optimized results of averaged coordination numbers at Al sites are listed in Table I, along with the density. It is noted that the atomic displacement from the classical MD position is less than 0.3 Å, and significant structural change does not exist between the classical MD and the first-principles. The re-optimized coordination numbers of 4.33 - 4.58 are also in the experimental range.

It is usually said that the amorphous structure may have short-range order and no long-range order. Such feature can be confirmed in a radial distribution function (RDF). Calculated RDF is consistent with previous

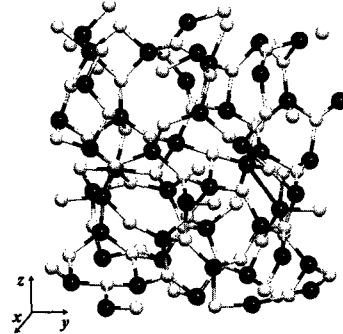


Fig.1: Calculated amorphous model structure of Al_2O_3 . Black and white circles show Al and O sites, respectively. This model contains 120 atoms in a unit cell. (see Table I)

classical MD results [15,16,17] and experiments [21]. There is a distinct peak around 1.8 Å corresponding to a nearest Al-O inter-atomic distance. And relatively low and broad peaks can be seen around 2.8 Å (nearest O-O) and 3.1 Å (nearest Al-Al). The Al-O distance is slight smaller than that in α -crystal (ca 1.9 Å). The results indicate that volume expansion of the amorphous Al_2O_3 is originated not from bond length extension but from coordination number lowering, comparing with a crystal.

3.2 Electronic Structure

Calculated electronic band structure of the amorphous model shows that the model has ionic and insulating nature as α - Al_2O_3 crystal does. The valence bands have significant O-p character with a width of 7.5 eV, while the conduction bands have Al-s character and more spatially extended.

The energy gap is listed in Table I with an observed one [22]. Calculated values of the a- Al_2O_3 are smaller than that of experiments. However, it is well known that DFT-LDA calculations usually underestimate an energy gap of experiment. For α - Al_2O_3 crystal, calculated and experimental energy gaps are 6.3 eV and 8.8 eV, respectively. An important point here is that the band gap reduction of a- Al_2O_3 relative to that of crystals. The calculated reduction is about 3 eV, which is in the experimental range of 2 - 4 eV. This reduction may be originated from the coordination number lowering that changes local ionic potential.

Table I: Density (ρ), averaged coordination number for Al site (C.N.) and band gap (E_g) of several amorphous model of Al_2O_3 .

System	ρ (g/cm^3)	C.N. of Al	E_g (eV)
60 atom	3.23	4.58	3.54
	3.10	4.33	3.58
	3.15	4.50	3.65
120 atom	3.27	4.50	3.77
Experiment	3.05 - 3.40	4.1 - 4.8	5.1 - 6.9

3.3 Dielectric Constant

For α - Al_2O_3 crystal, the calculated dielectric constant ($\epsilon_{xx}=\epsilon_{yy}=8.97$ and $\epsilon_{zz}=11.24$) is in good agreement with the experimental value (8.90 and 11.11) [4]. It is noted that the electron contribution ϵ^{ele} (2.88 and 2.84) is smaller than the lattice one ϵ^{lat} (6.09 and 8.40) as in other high-k materials. For a- Al_2O_3 (120 atoms/cell, see Tab.I and Fig.1), the calculated lattice dielectric tensor is

$$\epsilon^{\text{lat}} = \begin{pmatrix} 8.08 & -0.06 & 0.51 \\ -0.06 & 6.42 & 0.36 \\ 0.51 & 0.36 & 7.61 \end{pmatrix}.$$

Average of the diagonal components is 7.37, while the off-diagonal components are relatively small. In general, dielectric tensor should be diagonal and isotropic for ideal amorphous systems. Experimental dielectric constants are 8.3 – 11.0, and its electronic contribution are 2.50 – 2.79 [23]. By subtracting these values, the experimental lattice dielectric constant can be estimated as 5.5 – 8.5 that is consistent with the calculated result. We analyze Born effective charge and lattice vibration, as the same manner for amorphous ZrO_2 performed recently by *Zhao et al.* [24].

Calculated Born effective charge of diagonal average is shown in Fig.2. Most striking feature is that the values are almost ionic, namely roughly +3 and -2 for Al and O sites, respectively. To be precise, these are slight smaller than +3 and -2 within 0.5. Fig.3 (a) shows calculated phonon density of states (DOS) at Γ point. In order to specify phonon mode leading to the high dielectric constant, we calculated infra-red active phonon DOS as

$$D(\omega) = \sum_{\lambda} \left(\frac{Z_{\lambda}^2}{\omega_{\lambda}} \right)^2 \delta(\omega - \omega_{\lambda}),$$

that is shown in Fig.3 (b). It is clearly seen that there are much high densities at the low frequency in the range of 80 – 100 cm^{-1} .

Lattice dielectric constant can be decomposed as

$$\epsilon_{\alpha\beta}^{\text{lat}} = \sum_i \epsilon_{\alpha\beta}^{\text{lat}}(i),$$

here $\epsilon_{\alpha\beta}^{\text{lat}}(i)$ is contribution of i -th atomic site. The diagonal summation $\epsilon_{xx}^{\text{lat}}(i)+\epsilon_{yy}^{\text{lat}}(i)+\epsilon_{zz}^{\text{lat}}(i)$ is plotted in Fig.4. Although we cannot find the strong dependency on the atomic coordination number and atomic species, there are some atomic sites having high $\epsilon_{\alpha\beta}^{\text{lat}}(i)$ values as indicated in Fig.4 by Al(a)-(c) and O(a). These atomic sites with neighboring atoms are shown in Fig.5. It seems that the local atomic coordination is approximately “planer” environment. Actually, the component along z direction ($\epsilon_{zz}^{\text{lat}}(i)$) is quite high (ca 1.0), while other components are relatively small values (less than 0.2) for Al(a) and O(a) sites. Similarly, site-decomposed values are especially large along “plane-normal” direction for the Al(b) and Al(c) sites. We can conclude that the atomic sites with planer coordination especially contribute to the high lattice dielectric constant through low-frequency lattice vibration in a- Al_2O_3 .

In order to confirm the above results, we calculate the lattice dielectric constant for relatively small systems, namely a- Al_2O_3 with 60 atoms/cell (see Table I). Calculated values are also in that of the experimental range, and qualitatively similar conclusion is obtained.

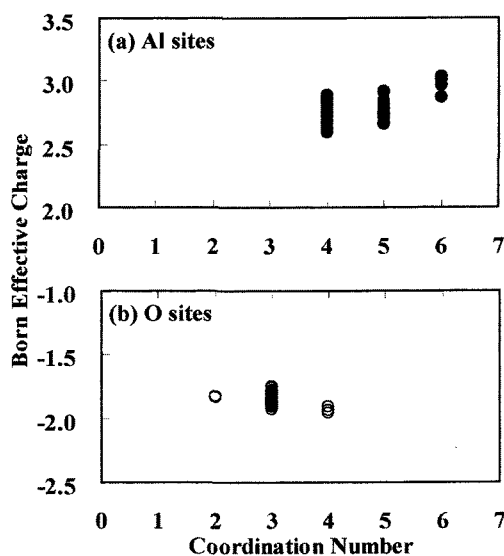


Fig.2: Calculated averaged Born effective charge ($(Z_{i,xx}^+Z_{i,yy}^+Z_{i,zz}^+)/3$) in a- Al_2O_3 model (120 atoms/cell) for (a) Al (solid circles) and (b) O (open circles) sites.

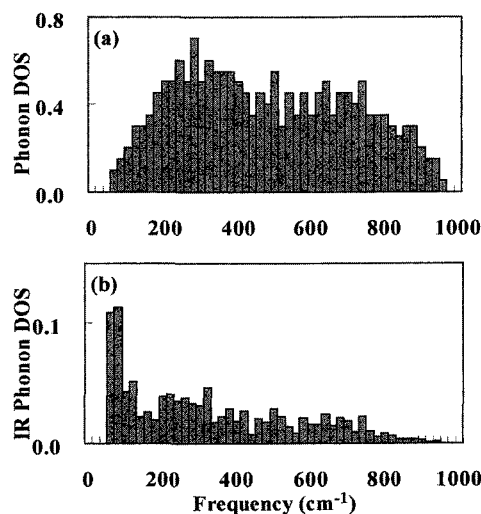


Fig.3: (a) Calculated phonon density of states and (b) infra-red active one $D(\omega)$ at Γ point in a- Al_2O_3 model (120 atoms/cell).

4. CONCLUSIONS

Structural, electronic and dielectric properties of amorphous Al_2O_3 are investigated from first-principles. Calculated density, coordination number and band gap are consistent with that of experimental results. These values are smaller than that in α - Al_2O_3 and other meta-stable crystals. Calculated dielectric constant is also in good agreement with observed values. As in the cases of other high-k materials, the contribution of lattice polarization is much larger than that of electron one. In the a- Al_2O_3 , some atomic sites having relatively small coordination number (such as having a planer local atomic environment) makes large contribution to the dielectric constant through the low-frequency lattice vibration mode.

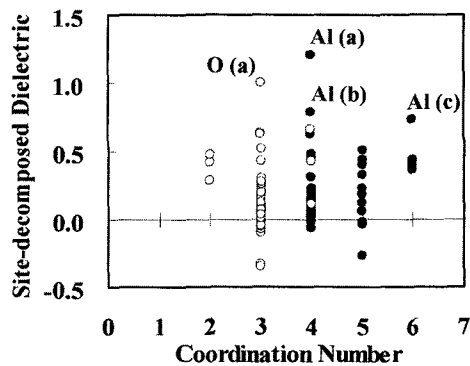


Fig.4: Site-decomposed lattice dielectric constant ($\epsilon_{xx}^{\text{lat}}(i) + \epsilon_{yy}^{\text{lat}}(i) + \epsilon_{zz}^{\text{lat}}(i)$) in $\alpha\text{-Al}_2\text{O}_3$ (120 atoms/cell). Solid and open circles show Al and O sites, respectively.

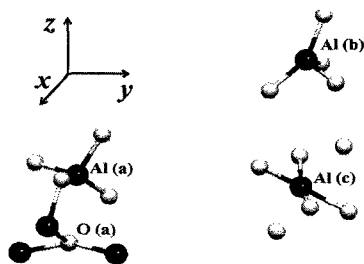


Fig.5: Local atomic structures causing high dielectric constant (see Fig.4) in $\alpha\text{-Al}_2\text{O}_3$ (120 atoms/cell). Black and white spheres denote Al and O atoms, respectively.

ACKNOWLEDGMENTS

The authors would like to thank Takahiro Yamasaki, Masakuni Okamoto and Kazuki Mae for invaluable discussions. The computation in this work has been performed by using Information Technology Center, University of Tokyo, Japan, and Supercomputing System, National Institute for Materials Science, Japan, and Information Technology Based Laboratory (ITBL), Japan. This research was done in "Frontier Simulation Software for Industrial Science (FSIS)" project supported by IT program of Ministry of Education, Culture, Sports, Science and Technology, Japan.

REFERENCES

- [1] Y. Sugiyama, S. Pidin and Y. Morisaki, *FUJITSU Sci. Tech. J.*, **39**, 94, (2003).
- [2] M. Koyama, Y. Kamimuta, M. Koike, M. Suzuki and A. Nishiyama, "Extended Abstracts of the 2003 International Conference on Solid State Devices and Materials", Tokyo (2003), pp.48-49.
- [3] Y. Tamura, Y. Sugiyama, M. Yamaguchi, H. Minakata, Y. Tanida, T. Sakoda, M. Nakamura and Y. Nara, "Extended Abstracts of the 2003 International Conference on Solid State Devices and Materials", Tokyo (2003), pp.54-55.
- [4] For example: T. Yamamoto, H. Momida, T. Hamada, T. Uda and T. Ohno, *Thin Solid Films* (2005) in press.
- [5] P. Hohenberg and W. Kohn, *Phys. Rev.* **136**, B864, (1964).
- [6] W. Kohn and L. J. Sham, *Phys. Rev.* **140**, A1133, (1965).
- [7] J. P. Perdew and Y. Wang, *Phys. Rev. B* **45**, 13244, (1992).
- [8] D. Vanderbilt, *Phys. Rev. B* **41**, 7892, (1990).
- [9] N. Troullier and J. L. Martins, *Phys. Rev. B* **43**, 1993, (1991).
- [10] <http://www.fsis.iis.u-tokyo.ac.jp>
- [11] M. Matsui, *Phys. Chem. Minerals*, **23**, 345, (1996).
- [12] S. Nosé, *Mol. Phys.* **52**, 255, (1984).
- [13] W. G. Hoover, *Phys. Rev. A* **31**, 1695, (1985).
- [14] M. Parrinello and A. Rahman, *J. App. Phys.* **52**, 7182, (1981).
- [15] C. Kaneta, Y. Kosaka and T. Yamasaki, "Semiconductor Technology (ISTC2002)", The Electrochemical Society, USA, 2002, pp.262-271.
- [16] T. Yamasaki and C. Kaneta, "Search for high-k gate dielectric materials of $\text{Al}_2\text{O}_3\text{-ZrO}_2\text{-HfO}_2\text{-SiO}_2$ systems by empirical molecular dynamics simulation (1)" (Article in Japanese).
- [17] G. Gutiérrez and B. Johansson, *Phys. Rev. B* **65**, 104202, (2002).
- [18] G. Harbeke, "Optical Properties of Semiconductors, Optical Properties of Solids", ed. F. Abeles, North-Holland, Amsterdam, (1972), pp.21-92.
- [19] R. D. King-Smith and D. Vanderbilt, *Phys. Rev. B* **47**, 1651, (1993).
- [20] R. Resta, *Rev. Mod. Phys.* **66**, 899, (1994).
- [21] For example: R. Manaila, A. Dévényi and E. Candet, *Thin Solid Films*, **116**, 289, (1984), Y. Oka, T. Takahashi, K. Okada and S. Iwai, *J. Non-Crystalline Solids*, **30**, 349, (1979), P. Lamparter and R. Kniep, *Physica B* **234-236**, 405, (1997), S. M. El-Mashri, R. G. Jones and A. J. Forty, *Philosophical Magazine A* **48**, 665, (1983), A. J. Bourdillon, S. M. El-Mashri and A. J. Forty, *Philosophical Magazine A* **49**, 341, (1984), S.-M. Lee, D. G. Cahill and T. H. Allen, *Phys. Rev. B* **52**, 253, (1995).
- [22] For example: S. Miyazaki, *J. Vac. Sci. Technol. B* **19**, 2212, (2001), A. M. Goodman, *J. Appl. Phys.* **41**, 2176, (1970).
- [23] For example: E. P. Gusev, E. Cartier, D. A. Buchanan, M. Gribelyuk, M. Copel, H. Okorn-Schmidt and C. D'Emic, *Microelectronic Engineering* **59**, 341, (2001), K. S. Shamala, L. C. S. Murthy and K. N. Rao, *Mater. Sci. and Engineering B* **106**, 269, (2003).
- [24] X. Zhao, D. Ceresoli and D. Vanderbilt, arXiv:cond-mat/0403131 v2 14Oct2004.

(Received December 23, 2004; Accepted April 28, 2005)